



# 1 **Assessment of nutrient cycling in an intensive mariculture** 2 **system**

3 Yanmin Wang<sup>1</sup>, Xianghui Guo<sup>1</sup>, Guizhi Wang<sup>1</sup>, Lifang Wang<sup>1</sup>, Tao Huang<sup>1</sup>, Yan Li<sup>1</sup>,  
4 Zhe Wang<sup>1</sup>, Minhan Dai<sup>1</sup>

5 <sup>1</sup> State Key Laboratory of Marine Environmental Science, College of Ocean and Earth Sciences, Xiamen  
6 University, Xiamen, 361102, China

7 **Correspondence:** Minhan Dai (mdai@xmu.edu.cn)

8 **Abstract.** Rapid expansion of mariculture during past decades has raised substantial concerns about  
9 impacts on the coastal environment, notably eutrophication. This study focuses on one of the world's  
10 highest density mariculture sites, Sansha Bay, Fujian Province, China, featuring integrated multi-trophic  
11 aquaculture practices involving croaker, kelp and oyster, based on examination of nutrient distributions  
12 and releases. A two-endmembers-mixing model showed significant addition of dissolved inorganic  
13 nitrogen (DIN;  $6.9 \pm 4.1 \mu\text{mol L}^{-1}$ ) and phosphorus (DIP;  $0.45 \pm 0.29 \mu\text{mol L}^{-1}$ ) associated with  
14 mariculture activities in spring 2020. A mass balance model estimated an annual release of N and P from  
15 cage fish farming systems fed with mixed trash fish feed and formulated feed of  $(2.42 \pm 0.15) \times 10^4$  tons  
16 and  $(5.33 \pm 0.37) \times 10^3$  tons, respectively. Of the total feed input,  $52.8 \pm 4.7 \%$  of DIN and  $33.0 \pm 3.7 \%$   
17 of DIP were released into seawater, values much higher than the riverine input and exchange with  
18 offshore coastal waters. A co-culture strategy involving kelp and oyster production in 2020 removed  
19  $(1.08 \pm 0.01) \times 10^3$  tons of N and  $(1.56 \pm 0.08) \times 10^2$  tons of P, respectively. Therefore, adjusting feed  
20 strategies and improving feed conversion rates could alleviate eutrophication caused by mariculture  
21 expansion in this ecosystem.

## 22 **1 Introduction**

23 The global demand for aquatic products during past decades has fueled the rapid development of coastal  
24 aquaculture, making it the fastest growing sector of food production worldwide (Chen and Qiu, 2014;  
25 Subasinghe et al., 2009). Global aquaculture production has increased by approximately 600 %, from  
26 17.3 million tons (MT) in 1990 to 120.1 MT in 2019 (Fao, 2021). Mariculture accounts for ~48 % of  
27 total aquaculture production with a growth rate of  $2.36 \times 10^6$  tons  $\text{yr}^{-1}$ , which outcompetes that of  
28 freshwater culture ( $1.92 \times 10^6$  tons  $\text{yr}^{-1}$ ) over the past decade (Fao, 2021). Notably, China emerged as the



29 largest global aquaculture producer since 1989, contributing to ~57 % of total world production in 2019,  
30 i.e., a tenfold increase over the past two decades (Fao, 2021). This growth trend is expected to continue  
31 globally, most notably in developing countries (Diana et al., 2013).

32 Mariculture development has provided great economic and social benefits; the environmental impacts  
33 of using formulated and trash fish feeds are of critical concern (Cao et al., 2015; Cao et al., 2017). Cage  
34 farming for example, has been reported to contribute additional pressures to the already impacted coastal  
35 marine environment (Chopin et al., 2001; Dai et al., 2023). Many studies have reported eutrophication  
36 in waters used for mariculture (Bouwman et al., 2013; Schneider et al., 2005; Wang et al., 2012;  
37 Skriptsova and Miroshnikova, 2011). While the causes of eutrophication may be complex, they are often  
38 attributed to the low utilization efficiency of fish feeds (Nederlof et al., 2021). Although the Norwegian  
39 salmon farming industry has taken important steps to reduce nutrient release, such as the optimization of  
40 feed composition and improvement of the feed conversion rate (FCR), which has attained a range of  
41 1.06-1.17. However, such FCR values still translate into the release into the environment of 58 %-62 %  
42 nitrogen (N), 79 %-81 % phosphorus (P) and 58 %-62 % carbon (C) of the total feed input (Wang and  
43 Olsen, 2023). These unutilized nutrients can accumulate in both the water and sediment, eventually  
44 altering the aquatic and sedimentary environment, especially in closed and semi-closed bays where water  
45 exchange is limited. Consequently, harmful algal blooms (HABs) and seasonal hypoxia frequently occur  
46 in these coastal waters (Anderson et al., 2002; Aure and Stigebrandt, 1990; Li et al., 2014b; Breitburg et  
47 al., 2018). Mariculture can also result in varying environmental impacts. Thus, He et al. (2022) reported  
48 that suspended aquaculture weakens the onshore current near the aquaculture boundary and upwelling  
49 within the offshore aquaculture area, resulting in a reduction of ~60 % in the nutrient supply. Therefore,  
50 the effects of mariculture systems on coastal nutrient dynamics still remain inconclusive and  
51 quantitatively uncertain.

52 A novel development in the mariculture sector to increase its sustainability is to adopt an integrated  
53 multi-trophic aquaculture (IMTA) approach (Jiang et al., 2012; Granada et al., 2016; Chopin et al., 2012;  
54 Campanati et al., 2021; Wu et al., 2015; Wei et al., 2017). Macroalgal cultivation is often included in  
55 IMTA systems to alleviate environmental impacts, as it allows efficient nutrient recycling and  
56 transformation, because of its pronounced nutrient absorption and storage capacity in tissues, while also  
57 offering an ecologically friendly option (Yang et al., 2006; Marinho-Soriano et al., 2009). Bivalve



58 suspension-feeders provide another effective trophic pathway for the removal of suspended particulates  
59 and phytoplankton from the water in IMTA systems, leading to the conversion of nutrients into biomass  
60 (Martinez-Porchas and Martinez-Cordova, 2012; Carboni et al., 2016). However, the IMTA system is a  
61 complex ecosystem, in which the efficiency of nutrient removal by macroalgae and nutrient addition  
62 from fish cage farming depend on the feed type, the species under cultivation and the feeding strategy,  
63 variables which have generally not been fully studied. It is thus crucial to assess nutrient cycling in IMTA  
64 systems, and determine the nutrient budget by also considering other sources of nutrients, as these have  
65 important policy implications (Campanati et al., 2021; Carballeira Braña et al., 2021).

66 We here focus on Sansha Bay located in Fujian Province, China, one of the highest density IMTA  
67 system worldwide, featuring the world's largest croaker (*L. crocea*) cage culture as a case study to shed  
68 light on the interactions between a mariculture system and the environment (Song et al., 2023).  
69 Production of this fish species accounts for 72.3 % of total fish aquaculture production in Sansha Bay,  
70 requiring millions of tons of feed annually (Xie et al., 2020). Therefore, the development of this  
71 mariculture industry and the associated use of feeds might be a major contributor to nutrient pollution in  
72 this bay. However, to date, little is known about how the N and P budgets in the fish farming system are  
73 affected by different types of feeds. Finally, the role of macroalgae and bivalve mollusks in nutrient  
74 removal in Sansha Bay remains unknown.

75 This study aims to provide a scientific basis for assessing the role of mariculture as a driver of changes  
76 in the coastal environment and proposes to support science-based decision-making for transforming the  
77 mariculture activities in coastal waters into a more sustainable model. We examine semi-quantitatively  
78 the variation in nutrient characteristics in spring. Subsequently, we establish a mass balance of N and P  
79 to assess the release of nutrients from fish farming systems using different feeds. We also analyze the  
80 external nutrient input/removal in this ecosystem that is affected by intensive mariculture (fish, kelp and  
81 oyster farming), riverine input and exchange with offshore coastal waters.

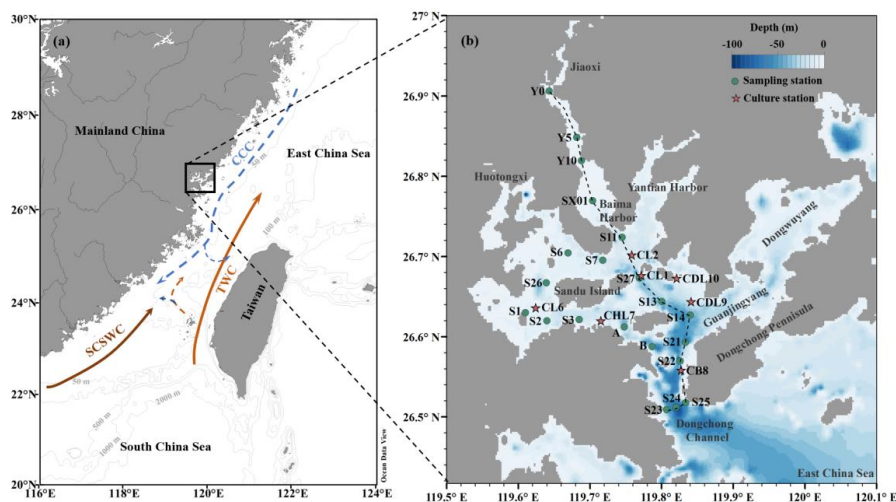
## 82 **2 Materials and methods**

### 83 **2.1 Study area and maricultural practices**

84 Sansha Bay, located on the northeast coast of Fujian Province, China, is a semi-enclosed bay comprised  
85 of several secondary bays, such as Baima Harbor, Yantian Harbor, Dongwuyang, Guanjingyang, and



86 Sandu'ao (Fig. 1) (Lin et al., 2017a). The surface area of the bay is  $\sim 675 \text{ km}^2$  (Lin et al., 2016), with a  
87 tortuous 553 km coastline (Yan and Cao, 1997). It has only one outlet, ca. 2.9 km wide, to the southern  
88 East China Sea (ECS) (Wang et al., 2018). Due to its geographical features, Sansha Bay has historically  
89 served as a natural sheltered bay (Lin et al., 2017a), that fostered the vigorous development of the  
90 mariculture industry (Xie et al., 2020; Wei et al., 2017; Wu et al., 2015). Sansha Bay is surrounded by  
91 mountains with outcroppings of medium acidic volcanic rocks (Yan and Cao, 1997). It receives several  
92 mountain rivers, among which the Jiaoxi and Huotongxi Streams provide the largest runoff. The annual  
93 freshwater discharge of the Jiaoxi Stream is  $6.97 \times 10^{10} \text{ m}^3$  (Huang and Ding, 2014), while that of the  
94 Huotongxi Stream is  $2.73 \times 10^9 \text{ m}^3$  (Li et al., 2014a). The bay is characterized by strong semidiurnal tides,  
95 with an average tidal range exceeding 5 m (Lin, 2014). The tidal prism is  $\sim 2.68 \times 10^9 \text{ m}^3$  (Wang et al.,  
96 2011), and the water depth within the bay ranges from a few meters to 90 m. The region experiences  
97 prevailing seasonal monsoons, influenced by the winter northeast wind and summer southwest wind. As  
98 a result, the Bay water is a dynamic mixture of the China Coastal Current (CCC), the Taiwan Warm  
99 Current (TWC), and the South China Sea Warm Current (SCSWC), with seasonal variation in their  
100 proportions (Xu and Xu, 2013; Wang et al., 2018; Yang et al., 2008; Huang et al., 2019). The unique  
101 natural geomorphology and intensive mariculture activities have influenced the flow field and water  
102 exchange in Sansha Bay. Cage aquaculture weakens the overall flow within the bay, but appears to  
103 strengthen the water flow among individual cages (Lin et al., 2019), while the difference in residual water  
104 level between the outer and inner bay is more influenced by cross-shore winds (Lin et al., 2017b).  
105 Moreover, the seawater half-exchange time in the main channel is less than 10 days, while it exceeds 30  
106 days at the head of the bay (Wu et al., 2015; Lin et al., 2017a; Lin et al., 2019).

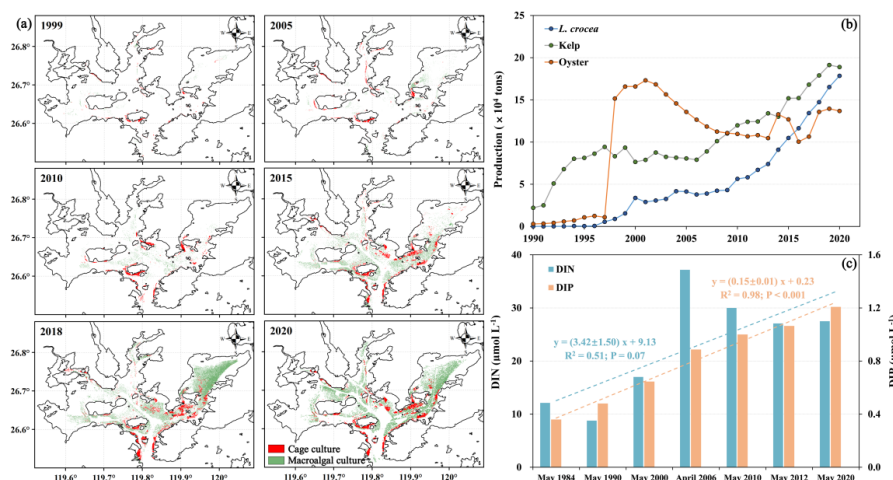


107  
108 **Figure 1. (a) Map of the study area and schematic of local currents. Bathymetric data reflect the latest General**  
109 **Bathymetric Chart of the Oceans (GEBCO) grid data. Blue dashed lines, red and brown solid lines represent**  
110 **the China Coastal Current (CCC), Taiwan Warm Current (TWC) and South China Sea Warm Current**  
111 **(SCSWC). (b) Sampling stations (dark green circles) in Sansha Bay during May 2020. Also shown are**  
112 **mariculture zones (red stars). Jiaoxi and Huotongxi are two main streams discharging into Sansha Bay.**

113 Aquaculture activities utilize ~69 % of Sansha Bay's area. The main cultured species include the *L.*  
114 *crocea*, oyster (*C. angulate*), kelp (*L. japonica*), and others. Cages used in shallow and deep-water have  
115 an area of  $4.5 \times 10^6 \text{ m}^2$  and  $1.39 \times 10^6 \text{ m}^3$ , respectively as of 2020 (data from Xingchun Wang, Min Dong  
116 Fisheries Research Institute, Fujian Province). Specifically, the farming densities for fish 100-200 g and  
117 500 g wet weight approach ca. 600 and 160 fish  $\text{m}^{-2}$ , respectively (Liu et al., 2022). Trash fish feeds  
118 constitute the primary bait for breeding *L. crocea*, accounting for ca. 80 % of the feed source (Song et  
119 al., 2023). Based on remote sensing data from 1999 to 2020 (detailed in supplementary text S1),  
120 mariculture gradually expanded from nearshore to offshore waters. Cage culture began sporadically  
121 around several islands in deep-waters as early as 1999 and then expanded linearly and widely in the  
122 nearshore and surrounding areas, while macroalgal culture was scattered throughout the region in 2020  
123 (Fig. 2(a)). The productions of *L. crocea* and kelp were gradually increasing in the marine area off Ningde  
124 City (production data from the Statistical Yearbooks of Ningde City,  
125 <http://tjj.ningde.gov.cn/xxgk/tjxx/tjnj/>). The total production of *L. crocea* increased from 56 tons in 1990  
126 to  $1.785 \times 10^5$  tons in 2020. Due to differences in the statistical methodology for *L. crocea* and oyster (the  
127 latter includes the shell weight) since 1997, oyster production showed a linear increase (Fig. 2(b)). A  
128 synthesis of literature data(Cai, 2007; Zheng, 2017; Liu, 2013; Wang et al., 2009) reveals that nutrient



129 concentrations increased steadily from 1984 to 2020, with an annual mean growth rate of  $3.42 \pm 1.50$   
130  $\mu\text{mol L}^{-1}$  for dissolved inorganic nitrogen (DIN) and  $0.15 \pm 0.01 \mu\text{mol L}^{-1}$  for dissolved inorganic  
131 phosphorus (DIP). Thus, DIN and DIP concentrations have increased more than two and three folds,  
132 respectively, since the 1980s (Fig. 2(c)).



133  
134 **Figure 2. (a) Classification of cage culture and macroalgal culture in Sansha Bay from 1999 to 2020 based on**  
135 **Lansat and Sentinel-2 remote sensing data used to perform support vector machine (SVM) classification, in**  
136 **which red represents cage culture and green represents macroalgal culture. (b) Changes in annual production**  
137 **of *L. crocea*, kelp and oyster from 1990 to 2020. (c) Dissolved inorganic nitrogen (DIN) and phosphorus (DIP)**  
138 **concentrations in Sansha Bay from 1984 to 2020. Light blue and orange dashed lines represent the linear**  
139 **regression lines over time of DIN and DIP concentrations, respectively; linear regression equations are also**  
140 **shown ( $R^2$  = coefficient of determination).**

141 **Notes:** Nutrient 1984 data are from the *National Comprehensive Survey of Coastal Zone and Tiled Resources*;  
142 1990 data are from volume 7 of *Gulf Annals of China*; 2000 data are from Cai (2007); 2006 data are from  
143 Wang et al. (2009); 2010 data are from Liu (2013); 2012 data are from Zheng (2017); 2020 data are from this  
144 study. Due to the lack of data in May 2006, the substitution of April data could be a potential reason for the  
145 elevated DIN concentration.

## 146 2.2 Sampling and methods of analysis

147 The research cruise was conducted onboard the R/V *Funing II* during May 18-28, 2020. Water  
148 temperature and chlorophyll *a* (Chl-*a*) concentrations were measured continuously using a multi-  
149 parameter instrument (YSI Model 5065, YSI Co., USA). Discrete water samples for salinity (S)  
150 determination were collected using Niskin bottles and analyzed in the laboratory using a portable  
151 salinometer (Model Multi 340i, WTW Co., Germany). Simultaneously, water samples for analysis of



152 nitrate ( $\text{NO}_3^-$ ), nitrite ( $\text{NO}_2^-$ ), ammonium ( $\text{NH}_4^+$ ), phosphate ( $\text{PO}_4^{3-}$  or DIP), and silicate ( $\text{Si}(\text{OH})_4$ )  
153 concentrations were taken and filtered through a 0.45  $\mu\text{m}$  pore size cellulose acetate membrane filter into  
154 125 mL high density polyethylene plastic bottles.

155 Nutrient samples, except those for  $\text{Si}(\text{OH})_4$ , were frozen onboard and then measured at a land-based  
156 laboratory in Xiamen University. Samples for  $\text{Si}(\text{OH})_4$  analysis were preserved with 100  $\mu\text{L}$  of  
157 chloroform and were refrigerated at 4  $^\circ\text{C}$  until analysis. Nutrient concentrations were measured using an  
158 Auto Analyzer 3 (AA3) instrument (Bran+Luebbe, Germany) with a detection limit of 0.04  $\mu\text{mol L}^{-1}$  for  
159  $\text{NO}_2^-$ , 0.1  $\mu\text{mol L}^{-1}$  for  $\text{NO}_2^- + \text{NO}_3^-$ , 0.08  $\mu\text{mol L}^{-1}$  for  $\text{PO}_4^{3-}$  and 0.16  $\mu\text{mol L}^{-1}$  for  $\text{Si}(\text{OH})_4$ .  $\text{NH}_4^+$   
160 concentrations were determined using an integrated syringe-pump-based environmental-water analyzer  
161 (iSEA) based on the improved indigo phenol blue spectrophotometric method, with a detection limit of  
162 0.15  $\mu\text{mol L}^{-1}$  (Li et al., 2019). Samples for total alkalinity (TA) analysis were stored in 250 mL PYREX®  
163 borosilicate glass bottles and preserved with 250  $\mu\text{L}$  of saturated  $\text{HgCl}_2$  solution (Guo and Wong, 2015).  
164 Total alkalinity was measured using potentiometric titration with 0.1  $\text{mol L}^{-1}$  hydrochloric acid, and  
165 certified reference material for carbon dioxide from Andrew G. Dickson (the Scripps Institution of  
166 Oceanography, University of California, San Diego, USA) was adopted to standardize measurements  
167 (Cai et al., 2004). Both precision and accuracy were  $\pm 2 \mu\text{mol kg}^{-1}$ . Dissolved oxygen (DO) concentration  
168 from discrete water samples was measured onboard using the spectrophotometric Winkler method  
169 (Labasque et al., 2004). Meanwhile, biological samples were also collected, such as those of *L. crocea*,  
170 kelp, oyster and fish feed, which were freeze-dried and used for analysis of N and P components ( $C_{\text{N,P}}$ ).  
171  $C_{\text{N}}$  was determined using an elemental analyzer (Model Vario EL cube, Elementar Co., Germany), while  
172  $C_{\text{P}}$  was analyzed using an AA3 analyzer after ashing the samples.

### 173 2.3 Endmember mixing model

174 A two-endmember mixing model was used to construct the conservative mixing schemes between  
175 different water masses based on the TA-S diagram and to quantify the addition or removal of nutrients  
176 on top of conservative mixing (Fig. 3a) because TA is assumed to be quasi-conservative in the absence  
177 of organic matter production/degradation and the exclusion of biogenic calcium carbonate  
178 production/dissolution processes (Zhai et al., 2014; Zhao et al., 2020). Given that freshwater discharge  
179 into the bay mainly occurs via the Jiaoxi Stream, we selected station Y0, located at the most upstream of  
180 the surveyed section of the Jiaoxi, with a salinity of 0.3 and high nutrient concentrations, as the optimal



181 candidate for the freshwater endmember, represented by the symbol “FW”. The seawater endmember is  
 182 defined as East China Sea offshore water, represented by the subscript “SW”. The average value of station  
 183 S25 characterized by high salinity and low nutrient concentrations was selected as the seawater  
 184 endmember. Therefore, the mixing model is based on mass balance equations for S and the water  
 185 fractions (f), as follows:

$$186 \quad f_{FW} + f_{SW} = 1, \quad (1)$$

$$187 \quad f_{FW} \times S_{FW} + f_{SW} \times S_{SW} = S_{meas}, \quad (2)$$

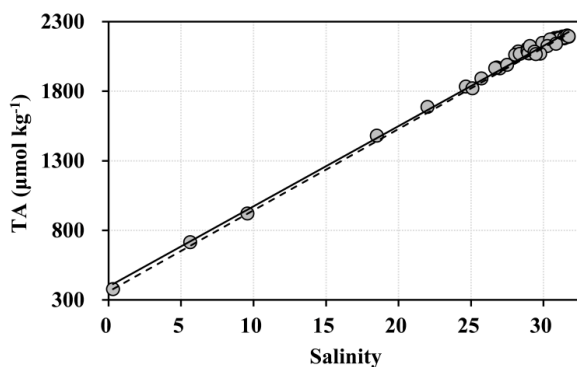
188 Based on the percent contribution of various water masses, the predicted conservative concentrations  
 189 of nutrients ( $Nutrient_{pre}$ ) could be calculated by Eq. (3). The difference between the field measured value  
 190 ( $Nutrient_{meas}$ ) and the predicted conservative value was denoted as  $\Delta$  ( $\Delta Nutrient$ , i.e.,  $\Delta DIN$ ,  $\Delta DIP$ , and  
 191  $\Delta Si(OH)_4$ ), reflecting the amount of nutrient production (positive) or removal (negative) associated with  
 192 non-mixing processes:

$$193 \quad Nutrient_{pre} = Nutrient_{FW} \times f_{FW} + Nutrient_{SW} \times f_{SW}, \quad (3)$$

$$194 \quad \Delta Nutrient = Nutrient_{meas} - Nutrient_{pre}, \quad (4)$$

195 where  $Nutrient_{FW}$  and  $Nutrient_{SW}$  represent the nutrient concentrations of the two endmembers,  
 196 respectively.

197



198

199 **Figure 3. Total alkalinity (TA) versus salinity (S) diagram at all Sansha Bay stations. The solid black line**  
 200 **represents the fitted linear regression line, and the dashed black line represents the conserved mixing line of**  
 201 **freshwater and seawater endmembers.**





#### 202 2.4 Mass balance of N and P in fish farming systems

203 Nitrogen and phosphorus budgets were established based on a mass balance principle (Wang et al., 2012;  
204 Olsen and Olsen, 2008); parameter values in the model are listed in Table S1. In the context of fish  
205 farming, the total amount of feed input (I) is equivalent to the sum of assimilated feed by fish (A) and  
206 the total waste discharge (L). It should be emphasized that waste emission from a fish farming operation  
207 is distinct from that of individual fish due to the loss of feed as particulates and the occurrence of fish  
208 mortality. In our calculations, we assumed that mortality is insignificant because dead fish are usually  
209 removed directly. Thus, the budget was calculated as:

$$210 \quad I = A + L, \quad (5)$$

211 The amount of N and P in feed input ( $I_{N,P}$ ) was obtained by multiplying fish production ( $P_f$ ), by the  
212 feed conversion ratio (FCR), and the N and P content of feed ( $C_{N,P}$ ):

$$213 \quad I_{N,P} = P_f \times FCR \times C_{N,P}, \quad (6)$$

214 The feed loss (L) is associated with a different feed loss ratio (LR) in the different feeding systems.  
215 Feed losses previously represented a relatively important source of particulate waste from fish farming,  
216 but feeding is currently better controlled such that losses are lower than in the past. In our calculations,  
217 20 % of fish production was fed with formulated feed, with an LR of  $4 \pm 1.4$  % (Bureau et al., 2003;  
218 Corner et al., 2006; Cromey et al., 2002); while 80 % of production was fed with conventional trash fish  
219 with an LR of 13 % (Qi et al., 2019).

220 The mass balance for individual fish ( $f$ ) can be represented by:

$$221 \quad I_f = A_f + F_f = G_f + E_f + F_f, \quad (7)$$

222 where  $I_f$  is the food intake, equal to total assimilation (i. e.,  $A = I - L$ ),  $F_f$  is feces production.  $A_f$  is food  
223 assimilation, which can be calculated from the food intake and assimilation efficiency ( $AE$ ) as  $A_f = I_f \times$   
224  $AE$ . Food assimilation consists of two parts,  $G_f$  and  $E_f$ , where  $G_f$  represents somatic growth or retention  
225 in biomass that can be calculated as fish production multiplied by the N and P content in fish ( $G_f = P_f \times$   
226  $C_{N,P}$ ), and  $E_f$  is excretion through urine discharge. Nitrogen and P are excreted mainly in the form of  
227 ammonium released at the gills and  $PO_4^{3-}$  in urine, respectively. The amount of  $E_f$  is equal to the amount  
228 of nutrients assimilated minus that retained in fish biomass. Excreted N and P are released into the  
229 environment in dissolved inorganic form, while N and P from uneaten feed and feces are released as



230 particulate organic nitrogen (PON-Feed and PON-Fecal) and particulate organic phosphate (POP-Feed  
231 and POP-Fecal), respectively. Approximately 15 % of particles will be dissolved in organic form  
232 (dissolved organic nitrogen, DON, and dissolved organic phosphate, DOP, respectively) according to  
233 Chen et al. (2003) and Sugiura et al. (2006).

## 234 **2.5 Kelp and oyster removal**

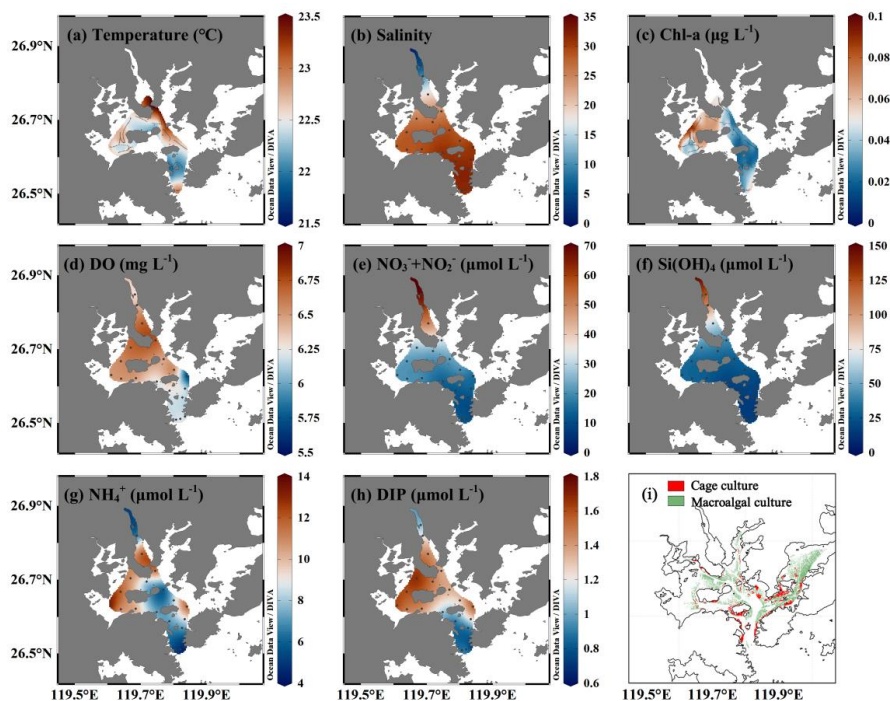
235 Kelp and oyster culture are effective in removing N and P from the environment. For kelp, the amount  
236 removed can be calculated as kelp production multiplied by the N and P content in kelp. For oysters, the  
237 amount removed includes the harvest of shell and soft tissue, which can be expressed as: removal =  
238 production × soft tissue ratio × soft tissue  $C_{N,P}$  + production × shell ratio × shell  $C_{N,P}$ .

## 239 **3. Results and discussion**

### 240 **3.1 Nutrient distribution in Sansha Bay**

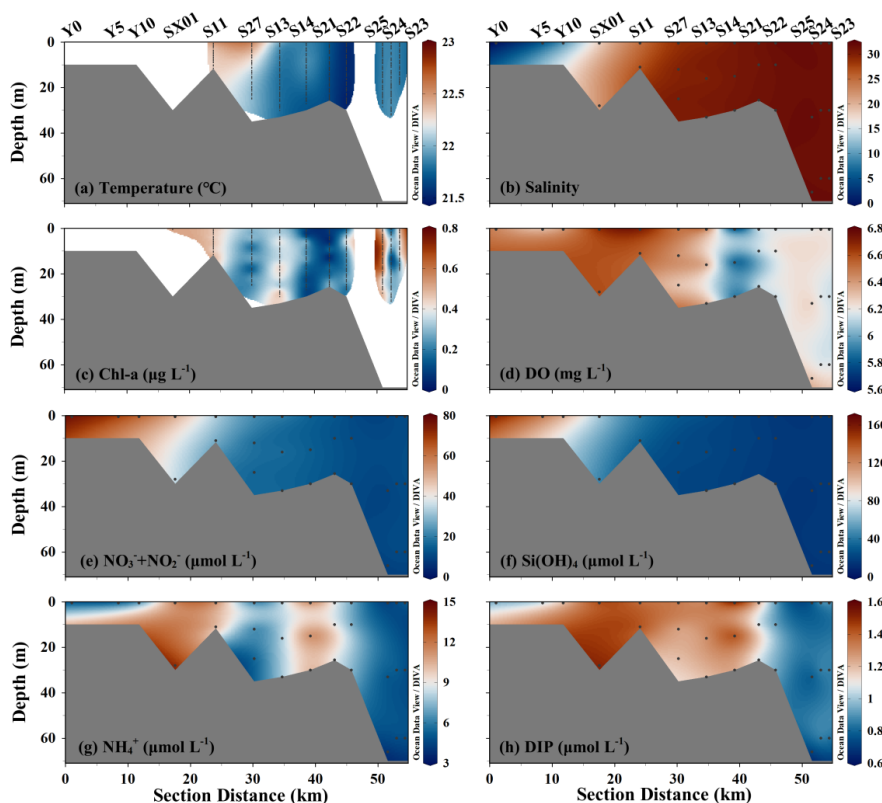
241 During late spring in Sansha Bay, the temperature showed a spatially variable distribution. It attained a  
242 maximum of 23.6 °C in Baima Harbor, upstream of the bay, while a lower temperature (~21.9 °C) was  
243 observed near the Dongchong Channel, at the Sansha Bay mouth (Fig. 4(a)). The salinity increased  
244 gradually from the inner bay to the mouth of the bay with values of 0.3 and 31.7 in the Jiaoxi Stream and  
245 the Dongchong Channel, respectively (Fig. 4(b)). Therefore, Sansha Bay is characterized by lower  
246 temperature and higher salinity at the mouth of the bay than upstream in the bay, mainly due to the  
247 influence of river runoff from the northwest of the bay and coastal ECS waters.

248 Nutrient concentrations generally decreased from the inner to outer portion of the bay. The highest  
249  $\text{NO}_3^- + \text{NO}_2^-$  and  $\text{Si}(\text{OH})_4$  concentrations, 76.1  $\mu\text{mol L}^{-1}$  and 153.5  $\mu\text{mol L}^{-1}$ , respectively, were found in  
250 the Jiaoxi Stream, and they decreased linearly with increasing salinity (Fig. 4(e) and (f)). The highest  
251 DIP and  $\text{NH}_4^+$  concentrations were not observed in the Jiaoxi Stream, but rather in waters near Sandu  
252 Island (stations S1, S2, S6 and S26) and Guanjingyang (station S14) (Fig. 4(g) and (h)), which may result  
253 from the release of fish feeds (Fig. 4(i)). Chl-*a* concentration were low (<0.1  $\mu\text{g L}^{-1}$ ) and uniform  
254 throughout the study area (Fig. 4(c)), indicating relatively low phytoplankton productivity.



255  
256 **Figure 4. Distribution of temperature, salinity, and concentrations of chlorophyll-*a* (Chl-*a*), dissolved oxygen**  
257 **(DO), nitrate + nitrite (NO<sub>3</sub><sup>-</sup>+NO<sub>2</sub><sup>-</sup>), silicate (Si(OH)<sub>4</sub> ammonium (NH<sub>4</sub><sup>+</sup>), and dissolved inorganic phosphorus**  
258 **(DIP) in surface waters in Sansha Bay (a-h). The distribution of macroalgae and cage culture in surface waters**  
259 **(i) is shown in green and red, respectively.**

260 The water was well-mixed throughout the water column, with only weak stratification in the estuarine  
261 plume, as shown in Fig. 5. Overall, nutrient concentrations followed a similar pattern to their distribution  
262 in the surface layer, with zonal variation from the inner to the outer portion of the bay. This may explain  
263 the absence of high Chl-*a* concentrations during the cruise due to weak stratification. The NO<sub>3</sub><sup>-</sup>+NO<sub>2</sub><sup>-</sup>  
264 concentration decreased from 62.4-76.1 µmol L<sup>-1</sup> at the river estuary to 9.3-11.9 µmol L<sup>-1</sup> at the  
265 Dongchong Channel, at the mouth of the bay; Si(OH)<sub>4</sub> concentrations exhibited a similar spatial  
266 distribution, gradually decreasing seaward. Lower concentrations were observed, however, near the  
267 Dongchong Channel, ranging from 0.71-0.92 µmol L<sup>-1</sup> for DIP, and 3.99-5.46 µmol L<sup>-1</sup> for NH<sub>4</sub><sup>+</sup>, except  
268 for the high values in Baima Harbor (Station SX01). Additionally, higher DIP and NH<sub>4</sub><sup>+</sup> concentrations  
269 as well as reduced DO levels were noted in station S14, which may result from organic matter  
270 remineralization.



271

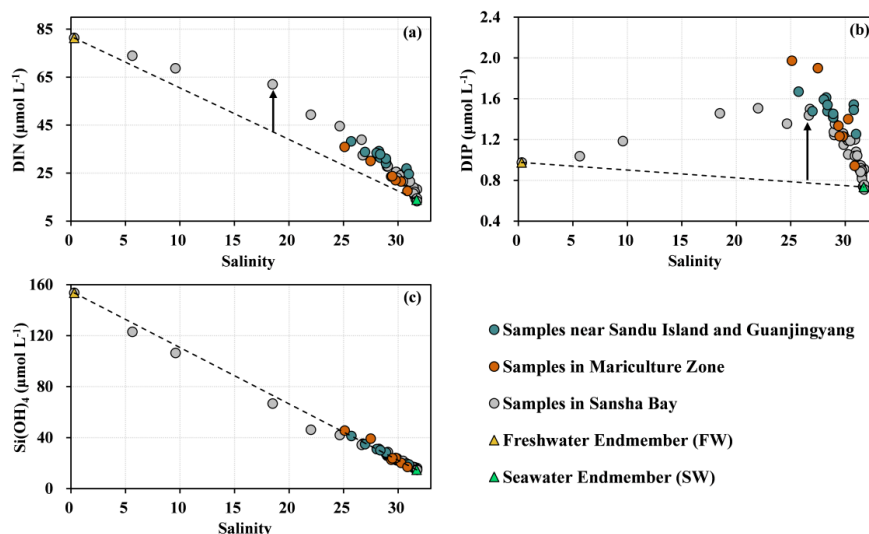
272 **Figure 5.** Distribution of temperature, salinity, and concentrations of chlorophyll-*a* (Chl-*a*), dissolved oxygen  
273 (DO), nitrate + nitrite ( $\text{NO}_3+\text{NO}_2$ ), silicate ( $\text{Si}(\text{OH})_4$ ), ammonium ( $\text{NH}_4^+$ ), and dissolved inorganic  
274 phosphorus (DIP) along the main section of Sansha Bay (a-h) from the Jiaoxi Stream (0 km) to the Dongchong  
275 Channel. Black circles within the transect indicate stations.

### 276 3.2 Nutrient changes due to biogeochemical processes and nutrient stoichiometric ratios

277 The DIN concentration gradually decreased with increasing salinity and exhibited obvious addition  
278 within the bay, attaining  $6.9 \pm 4.1 \mu\text{mol L}^{-1}$  ( $34.5 \% \pm 16.3 \%$ ) throughout the bay area. However, there  
279 was no anomalous enrichment near Sandu Island and the mariculture zone (Fig. 6(a)). However, the  
280 behavior of DIP differed in that the variation in DIP concentrations was more complex with a S value of  
281 25 as the boundary. We observed a  $58.8 \% \pm 37.0 \%$  ( $0.45 \pm 0.29 \mu\text{mol L}^{-1}$ ) DIP addition with a maximum  
282 addition of  $1.19 \mu\text{mol L}^{-1}$  in the mariculture zone. DIP concentrations gradually increased at  $S < 25$ , while  
283 they decreased when S exceeded 25. This pattern was likely induced by a buffering mechanism of DIP  
284 (Froelich, 1988), and/or may be attributable to variable feed flows in different zones (Fig. 6(b)).



285 Additionally, we observed that  $\text{Si(OH)}_4$  generally behaved conservatively with only minor removal.  
286 Although diatoms were dominant in this bay during spring, their abundance was relatively low, as  
287 indicated by the low Chl-*a* concentrations. As a result, individual stations deviated from the conservative  
288 mixed line at salinity below 25 (Fig. 6(c)).



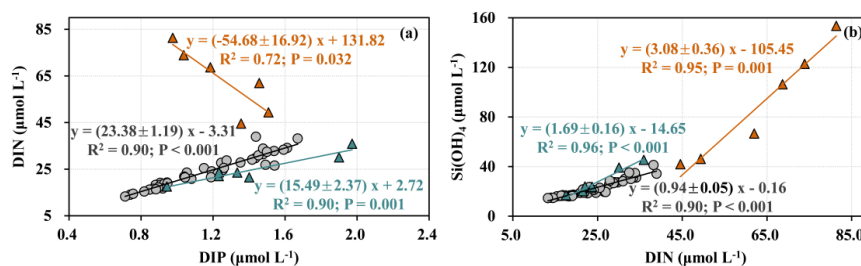
289  
290 **Figure 6. Relationship between nutrient concentrations vs. salinity in Sansha Bay in May 2020. Dark green,**  
291 **red and gray circles indicate stations near Sandu Island (station S1, S2, S6 and S26) and Guanjiyang**  
292 **(station S14), stations in the mariculture zone and freshwater and seawater endmember stations (yellow and**  
293 **green triangles). The black dashed line represents the conservative mixing line, and the black arrow indicates**  
294 **the obvious addition of dissolved inorganic nitrogen (DIN) and phosphorus (DIP) based on the conservative**  
295 **mixing lines.**

296 Overall, distinct DIN:DIP ratios associated with different water masses resulted in a variable effect on  
297 nutrient stoichiometry. Owing to the significant inflow of DIN from the Jiaoxi Stream, the plume water  
298 ( $S < 25$ ) exhibited a high DIN:DIP ratio. When the salinity was  $> 25$ , DIN and DIP showed a strong  
299 linear association with a ratio of  $23.38 \pm 1.19$  (Fig. 7(a)), which exceeded the Redfield ratio (Redfield et  
300 al., 1963), while, the DIN:DIP ratio in the mariculture zone was  $15.49 \pm 2.37$ , i.e., close to the Redfield  
301 ratio (Redfield et al., 1963), and consistent with previous observations in other mariculture waters in  
302 China (Bouwman et al., 2013). The  $\text{Si(OH)}_4$ :DIN ratio, however, exhibited different characteristics: in  
303 the plume region it was  $3.08 \pm 0.36$ , and thus significantly higher than the diatom absorption ratio of 1:1  
304 (Martin - Jézéquel et al., 2003; Brzezinski, 1985). This might be mostly due to weathering of volcanic  
305 rock, which is dominant in Ningde, and resulted in relatively high silicate concentrations. The



306  $\text{Si(OH)}_4$ :DIN ratio was approximately 1:1 in the region with salinity > 25, while it was  $1.69 \pm 0.16$  in the  
307 mariculture zone (Fig. 7(b)), which may be related to the lack of diatom dominance and preference for  
308 N in this region.

309 Results of the endmember mixing model showed significant DIN and DIP additions (positive values)  
310 at most stations. The  $\Delta\text{DIN}:\Delta\text{DIP}$  ratios in the study area were lower than the DIN:DIP ratios. Specifically,  
311 the  $\Delta\text{DIN}:\Delta\text{DIP}$  addition ratio was  $17.49 \pm 4.66$  at  $S > 25$  and  $7.91 \pm 1.48$  in the mariculture zone,  
312 indicating nutrient addition with a lower N:P ratio. There was no obvious pattern for the  $\Delta\text{Si(OH)}_4:\Delta\text{DIN}$   
313 ratio because  $\text{Si(OH)}_4$  is basically conservative in Sansha Bay. Given the intensity of mariculture activity  
314 in this bay, the lower  $\Delta\text{DIN}:\Delta\text{DIP}$  ratio may be related to bait feeding. Previous studies have shown that  
315 51 % of both N and P in bait were dissolved in water and the mass ratio of N and P was only 6.7 (Jia et  
316 al., 2003). Alternatively, this may be due to the addition of non-Redfield ratio nutrients from sediment.  
317 A study conducted in tidal flats of the Dutch Eastern Scheldt revealed that the DIN:DIP ratio in sediment  
318 porewater was notably lower than the Redfield ratio (Rios-Yunes et al., 2023).



319  
320 **Figure 7.** Dissolved inorganic nitrogen to phosphorus (DIN:DIP), and silicate to DIN ( $\text{Si(OH)}_4$ :DIN) ratios in  
321 Sansha Bay. Red triangles, gray circles and dark green triangles represent samples with salinity < 25, salinity >  
322 25 and the mariculture zone, respectively. Solid lines of the corresponding colors are the fitted linear  
323 regression lines. Linear regression equations are also shown.

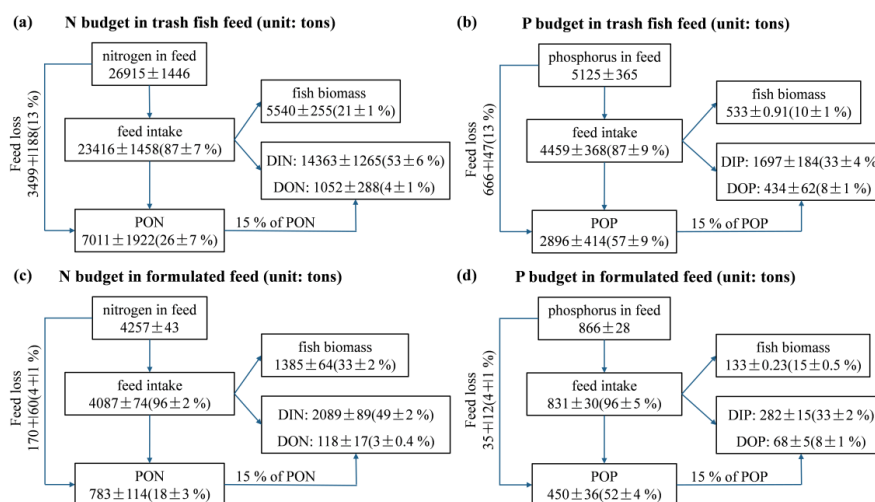
### 324 3.3 Nutrient release from the fish farming system

325 The production of *L. crocea* in 2020 reached  $1.785 \times 10^5$  tons (Statistical Yearbooks of Ningde;  
326 <http://tjj.ningde.gov.cn/xxgk/tjxx/tjnj/>). The N and P budget model for the cage system using both trash  
327 fish feed and formulated feed is shown in Fig. 8. Specifically, in the trash fish feed system, only  $21 \pm 1$  %  
328 of N and  $10 \pm 1$  % of P was incorporated into fish tissues, corresponding to  $(5.54 \pm 0.26) \times 10^3$  tons of N  
329 and  $(5.33 \pm 0.009) \times 10^2$  tons of P, and the remaining nutrients were released and lost to seawater or  
330 sediment (Fig. 8(a) and (b)). The N released to seawater was mainly excreted as DIN ( $53 \pm 6$  %), and  $26$   
331  $\pm 7$  % of N sank to the bottom as particulate organic nitrogen (PON) in the N budget model fed by trash



332 fish (Fig. 8(a)). In the P budget model, however, ca.  $(2.90 \pm 0.41) \times 10^3$  tons ( $57 \pm 9\%$ ) and  $(1.70 \pm$   
 333  $0.18) \times 10^3$  tons ( $33 \pm 4\%$ ) of P were lost as particulate organic phosphorus (POP) and DIP, respectively,  
 334 whereas about  $(4.34 \pm 0.62) \times 10^2$  tons of POP were released in the water column as DOP (Fig. 8(b)).

335 For the formulated feed system, only  $33 \pm 2\%$  of N and  $15 \pm 0.5\%$  of P in feed were absorbed and  
 336 utilized for incorporation in fish biomass. The remaining  $67 \pm 2\%$  of N ( $(2.87 \pm 0.08) \times 10^3$  tons) and  $85$   
 337  $\pm 4\%$  of P ( $(7.33 \pm 0.28) \times 10^2$  tons) were released into the water in both inorganic and organic form or  
 338 settled to bottom sediments (Fig. 8(c) and (d)). In the N budget model, about half of N ( $49 \pm 2\%$ ) was  
 339 lost as DIN (Fig. 8(c)). Similarly,  $52 \pm 4\%$  of P ( $(4.50 \pm 0.36) \times 10^2$  tons) was deposited as particulates in  
 340 the P budget model (Fig. 8(d)). Results indicated that the majority of the N waste generated by the fish  
 341 farming system was excreted as DIN, whereas the majority of P waste settled as POP. For both feeding  
 342 systems, the retention rate of N in fish biomass was higher than that of P, suggesting that fish excrete a  
 343 lower proportion of N than P. Additionally, the released DIN:DIP ratios showed inconsistencies. Molar  
 344 DIN:DIP ratios were  $\sim 18.72$  and  $\sim 16.39$  in the trash fish feed and formulated feed systems, respectively,  
 345 and thus quite consistent with the Redfield ratio (Redfield et al., 1963), which might partially explain the  
 346 variable  $\Delta$ DIN: $\Delta$ DIP ratios in the waters.

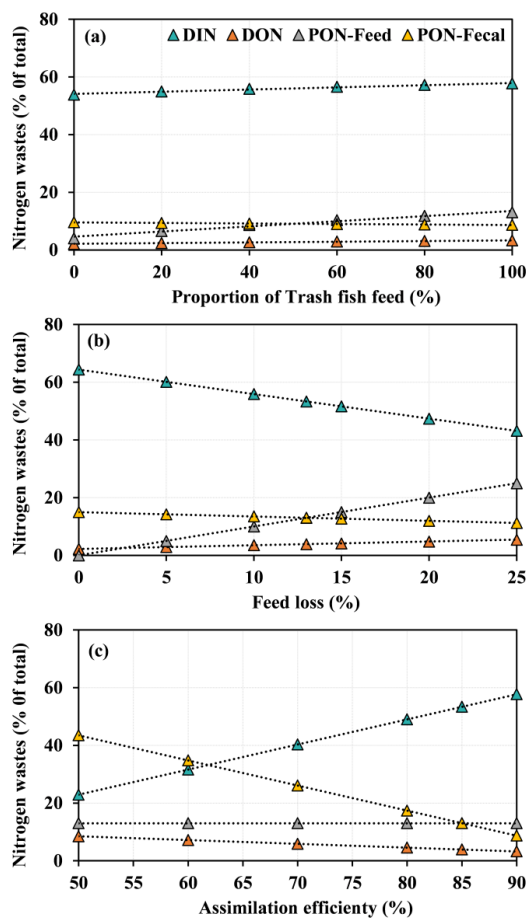


347  
 348 **Figure 8. Nitrogen (N; (a) and (c)) and phosphorus (P; (b) and (d)) budget for the cage systems using**  
 349 **formulated and trash fish feeds in Sansha Bay. Percentage values represent the proportion of each data to N**  
 350 **and P in feed. DIN and DIP: dissolved inorganic nitrogen and phosphorus, respectively; DON and DOP:**  
 351 **dissolved organic nitrogen and phosphorus, respectively; PON and POP: particulate organic nitrogen and**  
 352 **phosphorus, respectively.**



353 Our budget model showed that N and P released from the system fed by trash fish feed was much  
354 greater than that of the system fed by formulated feed due to the higher feed loss ratio in trash fish feed.  
355 Additionally, Fig. 9(a) demonstrates a progressive rise in the release of DIN and loss of PON-Feed with  
356 an increasing percent of trash fish feed, while DON and PON-Fecal were less variable. Therefore,  
357 formulated feed with varying particle size may be used for different fish sizes in comparison to the trash  
358 fish feed, which can reduce feed loss during farming. In addition, N and P retention rates of trash fish  
359 feed were lower than those of formulated feed. According to Verdegem et al. (1999), the higher feed  
360 protein content (generally higher in trash fish feed), the higher the proportion of N waste excreted.  
361 Moreover, the lower nutritional value and digestibility of trash fish feed may also explain its lower N  
362 retention rate (Hasan et al., 2016). The impacts of various feed losses and assimilation efficiencies are  
363 shown in Fig. 9(b) and (c). In the above calculations for the trash fish feed system, a 13 % feed loss value  
364 and 85 % N assimilation efficiency were used. The percentage of DIN excretion decreases as feed loss  
365 increases, and the percentage of combined organic waste from feed (PON-Feed) increases in a  
366 comparable manner (Fig. 9(b)). In contrast, a rise in the percent of DIN and a decline in the similarity  
367 between PON-Fecal are found with an increase in assimilation efficiency (Fig. 9(c)). Therefore, minor  
368 changes in feed loss and assimilation efficiency are unlikely to result in significant deviations in model  
369 predictions.





370  
 371 **Figure 9. Relationship between the percentage of nitrogen released and the proportion of trash fish feed (a, in**  
 372 **both feed systems), and feed loss rate (b, in the trash fish feed system) and assimilation efficiency (c, in the**  
 373 **trash fish feed system). The PON-Feed and PON-Fecal represent PON in feed and feces, respectively (PON:**  
 374 **particulate organic nitrogen). The dashed lines are fitted linear regression lines.**

### 375 3.4 Nutrient budget in Sansha Bay

376 In summary, only  $22.2 \pm 1.3$  % of N and  $11.1 \pm 0.7$  % of P was assimilated by cultured fish, resulting in  
 377 an annual release of  $(2.42 \pm 0.15) \times 10^4$  tons of N and  $(5.33 \pm 0.37) \times 10^3$  tons of P from the fish farming  
 378 system co-fed with trash fish feed and formulated feed. Furthermore,  $52.8 \pm 4.7$  % of DIN and  $33.0 \pm$   
 379  $3.7$  % of DIP was released into the water, and ca. half ( $47.5 \pm 6.6$  %) of the P settled to the bottom in  
 380 particulate form (Fig. 10).

381 To further clarify the nutrient contribution of the fish farming system to the water in Sansha Bay, we



382 estimated the nutrient (DIN and DIP) fluxes contributed by river discharge and exchange with offshore  
383 coastal waters based on the mass balance model (Gordon et al., 1996), as detailed in Supplementary Text  
384 S2. For example, the river discharge in May 2020 was  $71.3 \text{ m}^3 \text{ s}^{-1}$  (data from Nengwang Chen, Xiamen  
385 University). Results showed that the residual flow and the water exchange flux between the bay and  
386 offshore coastal water were  $-71.3 \text{ m}^3 \text{ s}^{-1}$  (negative values indicating outflow) and  $720.1 \pm 676.8 \text{ m}^3 \text{ s}^{-1}$ ,  
387 respectively (Table 1), which was also consistent with previous data ( $\sim 479.5 \text{ m}^3 \text{ s}^{-1}$ , unpublished data  
388 from Zhaozhang Chen, Xiamen University). Based on the water exchange rates and nutrient  
389 concentrations in different systems of this area, the DIN and DIP fluxes from the river were 2561 and 68  
390 tons  $\text{yr}^{-1}$ , respectively, while nutrient fluxes from the bay to the offshore coastal water were  $6229 \pm 6090$   
391 tons  $\text{yr}^{-1}$  for DIN and  $712 \pm 648$  tons  $\text{yr}^{-1}$  for DIP (Fig. 10). Due to the lack of field sediment data,  
392 biogeochemical processes at the sediment-water interface were not considered in the present study. As a  
393 result, without considering the contribution of sediment, the amount of dissolved inorganic nutrients  
394 (DIN and DIP) released by the fish farming system was much higher than that from river input. About  
395 32.8 % of the DIN and 34.8 % of the DIP were transported from Sansha Bay to offshore coastal waters  
396 through the Dongchong Channel.

397 Furthermore, by analyzing the N and P components in kelp and oysters, it can be determined that each  
398 ton of dried kelp can absorb 22.5 kg N and 3.5 kg P from seawater, while oyster soft tissue and shell can  
399 absorb 80.7 and 1.6 kg of N, and 5.6 and 0.44 kg of P, respectively. We thus estimated the removal of N  
400 and P by combining the production of macroalgae (kelp,  $1.888 \times 10^5$  tons) and bivalve mollusks (oysters,  
401  $1.368 \times 10^5$  tons) harvested in 2020 to assess nutrient removal by macroalgae and bivalve mollusks in the  
402 IMAT system. Our results showed that harvesting of kelp in Sansha Bay resulted in the removal of 708  
403  $\pm 3$  tons of N and  $110 \pm 8$  tons of P, respectively. In the case of oysters harvesting, it removed  $371 \pm 11$   
404 tons of N and  $46 \pm 0.1$  tons of P (Fig. 10). Therefore, the co-culture strategy removed  $(1.08 \pm 0.01) \times 10^3$   
405 tons of N and  $(1.56 \pm 0.08) \times 10^2$  tons of P in total. As a result, total emissions of N and P from mariculture  
406 in 2020 were  $(2.32 \pm 0.15) \times 10^4$  tons and  $(5.17 \pm 0.37) \times 10^3$  tons, respectively. Results showed that the  
407 amount of N and P released from feed was much higher than that of fish, macroalgae and oysters harvest  
408 combined. Thus, the release of feeds in the aquaculture system is the main cause of eutrophication when  
409 other nutrient sources remain constant in Sansha Bay.

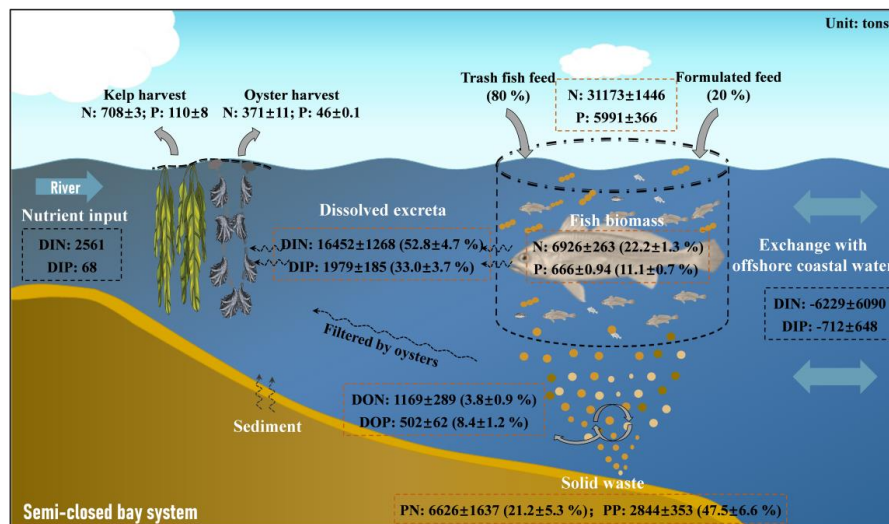
410 **Table 1. Summary of salinity (S), dissolved inorganic nitrogen and phosphorus concentrations (DIN and DIP,**  
411 **respectively, in  $\mu\text{mol L}^{-1}$ ), water discharge (V,  $\text{m}^3 \text{ s}^{-1}$ ) and calculated nutrient flux ( $F_{\text{DIN}}$  and  $F_{\text{DIP}}$ ,  $\text{mmol s}^{-1}$ ) in**



412 **the mass balance model.**

Salinity	$S_{riv}$	$S_{sys} \pm \sigma_{sys}$	$S_{oce} \pm \sigma_{oce}$	$S_{res} \pm u_{res}$
	0.3	$29.1 \pm 2.7$	$32.1 \pm 0.8$	$30.6 \pm 1.4$
DIN ( $\mu\text{mol L}^{-1}$ )	$DIN_{riv}$	$DIN_{sys} \pm \sigma_{DIN_{sys}}$	$DIN_{oce} \pm \sigma_{DIN_{oce}}$	$DIN_{res} \pm u_{DIN_{res}}$
	81.3	$27.5 \pm 9.0$	$9.7 \pm 2.8$	$18.6 \pm 4.7$
DIP ( $\mu\text{mol L}^{-1}$ )	$DIP_{riv}$	$DIP_{sys} \pm \sigma_{DIP_{sys}}$	$DIP_{oce} \pm \sigma_{DIP_{oce}}$	$DIP_{res} \pm u_{DIP_{res}}$
	0.98	$1.29 \pm 0.27$	$0.36 \pm 0.10$	$0.83 \pm 0.14$
V ( $\text{m}^3 \text{s}^{-1}$ )	$V_{riv}$	$V_{ex} \pm u_{ex}$		$V_{res}$
	71.3	$720.1 \pm 676.8$		-71.3
$F_{DIN}$ ( $\text{mmol s}^{-1}$ )	$F_{DIN_{riv}}$	$F_{DIN_{ex}} \pm u_{FDIN_{ex}}$		$F_{DIN_{res}} \pm u_{FDIN_{res}}$
	5800	$-12782 \pm 13789$		$-1327 \pm 335$
$F_{DIP}$ ( $\text{mmol s}^{-1}$ )	$F_{DIP_{riv}}$	$F_{DIP_{ex}} \pm u_{FDIP_{ex}}$		$F_{DIP_{res}} \pm u_{FDIP_{res}}$
	70	$-670 \pm 662$		$-59 \pm 10$

413 **Note:**  $S_{riv}$  represents the salinity of station Y0 in the Jiaoxi Stream;  $S_{sys}$  represents the average salinity in the  
 414 bay, excluding stations Y0, Y5, Y10 in the stream and S23, S24, S25 at the bay mouth;  $S_{oce}$  represents the  
 415 salinity of four stations (LJ21, LJ22, ND41 and ND42, not shown on the map) in offshore coastal waters;  $S_{res}$   
 416 represents the salinity of the residual flow;  $V_{riv}$ ,  $V_{res}$  and  $V_{ex}$  represent the river discharge, residual flow  
 417 discharge from the bay to offshore coastal waters and exchange flow between the bay and the offshore coastal  
 418 water, respectively;  $\sigma$  represents the standard deviation, and  $u$  represents the uncertainty associated with each  
 419 variable. Negative values indicate nutrient output.



420  
 421 **Figure 10.** Conceptual diagram illustrating the nutrient transformation of different species resulting from



422 mariculture in the semi-enclosed bay system, which was influenced by riverine and offshore coastal water  
423 exchange. Briefly, only a small proportion of the feed was consumed in support of fish growth, and the rest  
424 was released into the water in dissolved forms or settled to the seafloor in particulate forms. Mixed farmed  
425 kelp and suspension-feeding oysters can effectively remove nutrients from the water. The units in the figure  
426 are given in tons. Negative values indicate nutrient output. Nutrient abbreviations as in Fig. 8.

### 427 3.5 Strategies for the sustainable development of mariculture

428 This study has revealed important differences in the amount of nutrients released between fish farming  
429 systems depending on the use of different types of feeds. These differences may involve substantial  
430 variation in the FCR and feed composition among other factors. Specifically, the FCRs for formulated  
431 feed and trash fish feed were  $1.525 \pm 0.007$  and  $6.745 \pm 0.36$ , respectively (Gao et al., 2021; Qi et al.,  
432 2019). This indicates a notable 77.4 % increase in consumption when using trash fish feed compared to  
433 formulated feed, which requires an additional 5.22 tons of trash fish feed to produce one ton of *L. crocea*.  
434 As illustrated by the production in 2020,  $\sim 2.722 \times 10^5$  tons of formulated feed were required. In contrast,  
435 producing the same biomass of fish would demand  $1.204 \times 10^6$  tons of trash fish feed. Despite the much  
436 higher consumption of trash fish feed, consideration of feed cost (with the price of formulated feed at  
437  $1.0 \times 10^4$  RMB per ton and trash fish feed at  $1.2 \times 10^3$  RMB per ton (Shan et al., 2018)), the cost of  
438 formulated feed was higher by  $1.277 \times 10^3$  million RMB. Therefore, in practical terms, many farmers in  
439 Sansha Bay prefer to use the lower-cost trash fish feed. However, it is critical to note that as the proportion  
440 of trash fish feed usage increases, so does the release of DIN and PON-Feed into the environment can  
441 thus potentially have negative impacts on water quality. Improving the FCR to reduce feed usage and  
442 altering feed type and composition to lower costs are thus crucial for the sustainable development of fish  
443 farming systems, which has important policy implications.

444 However, the release of inorganic and organic nutrient waste is considered one of the major  
445 environmental challenges in fish farming in Sansha Bay. According to China's current seawater quality  
446 standards (GB3097-1997), water quality in Sansha Bay was classified as Grade III. While the occurrence  
447 of surface algal blooms and bottom oxygen depletion were infrequent in the inner bay, harmful algal  
448 blooms (HABs) were a recurring issue in the outer regions of the bay. Currently, there is no clear evidence  
449 linking the occurrence of HABs to the release of inorganic nutrients from fish cages. Nevertheless, water  
450 quality may become a critical factor leading to oxygen reduction and the occurrence of HABs in sensitive  
451 locations as mariculture production continues to increase. Although the government of Ningde took



452 measures to remove mariculture activities from the inner bay to the outer bay, it remains uncertain  
453 whether these measures will exacerbate HABs outbreaks outside the bay and reach a tipping point thus  
454 requiring long-term monitoring and research of water quality.

#### 455 **4 Conclusions**

456 The spatial variability of nutrients in the Sansha Bay was mainly controlled by the water mass mixing,  
457 between the riverine water and seawater, as well as the effects of mariculture system. Based on the end-  
458 member mixing model, we estimated that the additions of DIN and DIP during spring were  $\sim 6.9 \pm 4.1$   
459  $\mu\text{mol L}^{-1}$  and  $\sim 0.45 \pm 0.29 \mu\text{mol L}^{-1}$ , respectively. When using a mixture of formulated feed and trash  
460 fish feed at a 2:8 ratio in 2020, it was observed that approximately  $52.8 \pm 4.7\%$  of DIN and  $33.0 \pm 3.7\%$   
461 of DIP from the feeds were released into the surrounding waters, significantly surpassing the river input  
462 and exchange with offshore coastal water.

463 Up to now, methods for nutrient removal from eutrophic seawater are very limited. The cultivation  
464 and harvesting of macroalgae and bivalve mollusks provide an effective technology for nutrient removal.  
465 For each ton of kelp (dry weight) harvested, 22.5 kg N and 3.5 kg P can be removed from the water.  
466 Therefore, we recommend judicious planning of the proportions of macroalgae, oysters and fish farming.  
467 Additionally, when compared to formulated feed, the consumption of trash fish feed for producing one  
468 ton of fish increased by 77.4 %. Consequently, enhancing feed conversion rate, improving feed  
469 composition, and reducing feed costs are advantageous for the sustainable development of fish farming  
470 systems and lowering the risk of oxygen depletion and harmful algal blooms in sensitive areas.

471 *Data availability.* Data for temperature, salinity, DO, Chl-*a* and nutrients are available on the National  
472 Science Data Bank (<https://www.scidb.cn/en>). The productions of *L. crocea*, kelp and oyster from 1990  
473 to 2020 were obtained from the Statistical Yearbooks of Ningde City  
474 (<http://tjj.ningde.gov.cn/xxgk/tjxx/tjnj/>). The remote sensing data used to identify cage culture and  
475 macroalgal culture were obtained from Landsat (<https://glovis.usgs.gov/app>) and Sentinel-2  
476 (<https://scihub.copernicus.eu/dhus/#/home>).

477 *Supplement.*



478 *Author contributions.* YW and MD co-designed the study. YW, LW, TH, YL and ZW contributed to  
479 sampling, data acquisition and analysis. YW and MD analyzed and interpreted the data and drafted the  
480 manuscript. XG and GW revised the manuscript and made constructive comments.

481 *Competing interests.* The authors declare that they have no conflict of interests.

482 *Disclaimer.*

483 *Acknowledgements.* We thank the captain, crew and scientific staff of the R/V *Funing II* for their  
484 cooperation during the cruise, Kunning Lin for sample collection and ammonium analysis; Ai Qin Han  
485 for assistance in sample collection, Yi Xu for the collection of biological samples, Nengwang Chen and  
486 Xuwen Fang for providing the YSI and river discharge data, Junhui Chen for guidance in sample analysis,  
487 Haixia Guo for processing the remote sensing data, Yanping Xu and Feifei Meng for her logistical support.

488 *Financial support.* This research was funded by the National Natural Science Foundation of China  
489 (NSFC #42188102).

## 490 **References**

- 491 Anderson, D. M., Glibert, P. M., and Burkholder, J. M.: Harmful algal blooms and eutrophication:  
492 Nutrient sources, composition, and consequences, *Estuaries*, 25, 704-726,  
493 <https://doi.org/10.1007/BF02804901>, 2002.
- 494 Aure, J. and Stigebrandt, A.: Quantitative estimates of the eutrophication effects of fish farming on fjords,  
495 *Aquaculture*, 90, 135-156, [https://doi.org/10.1016/0044-8486\(90\)90337-M](https://doi.org/10.1016/0044-8486(90)90337-M), 1990.
- 496 Bouwman, L., Beusen, A., Glibert, P. M., Overbeek, C., Pawlowski, M., Herrera, J., Mulrow, S., Yu, R.,  
497 and Zhou, M.: Mariculture: significant and expanding cause of coastal nutrient enrichment,  
498 *Environmental Research Letters*, 8, 044026, <https://doi.org/10.1088/1748-9326/8/4/044026>, 2013.
- 499 Breitburg, D., Levin, L. A., Oschlies, A., Gregoire, M., Chavez, F. P., Conley, D. J., Garçon, V., Gilbert,  
500 D., Gutierrez, D., Isensee, K., Jacinto, G. S., Limburg, K. E., Montes, I., Naqvi, S. W. A., Pitcher, G.  
501 C., Rabalais, N. N., Roman, M. R., Rose, K. A., Seibel, B. A., Telszewski, M., Yasuhara, M., and  
502 Zhang, J.: Declining oxygen in the global ocean and coastal waters, *Science*, 359,  
503 <https://doi.org/10.1126/science.aam7240>, 2018.



- 504 Brzezinski, M. A.: The Si:C:N ratio of marine diatoms: interspecific variability and the effect of some  
505 environmental variables, *Journal of Phycology*, 21, 347-357, [https://doi.org/10.1111/j.0022-](https://doi.org/10.1111/j.0022-3646.1985.00347.x)  
506 [3646.1985.00347.x](https://doi.org/10.1111/j.0022-3646.1985.00347.x), 1985.
- 507 Bureau, D. P., Gunther, S. J., and Cho, C. Y.: Chemical composition and preliminary theoretical estimates  
508 of waste outputs of Rainbow Trout Reared in commercial cage culture operations in Ontario, North  
509 American Journal of Aquaculture, 65, 33-38, [https://doi.org/10.1577/1548-](https://doi.org/10.1577/1548-8454(2003)065<0033:CCAPTE>2.0.CO;2)  
510 [8454\(2003\)065<0033:CCAPTE>2.0.CO;2](https://doi.org/10.1577/1548-8454(2003)065<0033:CCAPTE>2.0.CO;2), 2003.
- 511 Cai, Q. H.: Study on main ecological environment of Sansha Bay in Fujian, *Environmental Monitoring*  
512 *in China*, 23, 101-105, <https://doi.org/10.19316/j.issn.1002-6002.2007.06.028>, 2007.
- 513 Cai, W.-J., Dai, M., Wang, Y., Zhai, W., Huang, T., Chen, S., Zhang, F., Chen, Z., and Wang, Z.: The  
514 biogeochemistry of inorganic carbon and nutrients in the Pearl River estuary and the adjacent Northern  
515 South China Sea, *Continental Shelf Research*, 24, 1301-1319,  
516 <https://doi.org/10.1016/j.csr.2004.04.005>, 2004.
- 517 Campanati, C., Willer, D., Schubert, J., and Aldridge, D. C.: Sustainable intensification of aquaculture  
518 through nutrient recycling and circular economies: more fish, less waste, blue growth, *Reviews in*  
519 *Fisheries Science & Aquaculture*, 30, 143-169, <https://doi.org/10.1080/23308249.2021.1897520>, 2021.
- 520 Cao, L., Naylor, R., Henriksson, P., Leadbitter, D., Metian, M., Troell, M., and Zhang, W.: China's  
521 aquaculture and the world's wild fisheries, *Science*, 347, 133-135,  
522 <https://doi.org/10.1126/science.1260149>, 2015.
- 523 Cao, L., Chen, Y., Dong, S., Hanson, A., Huang, B., Leadbitter, D., Little, D. C., Pikitch, E. K., Qiu, Y.,  
524 Sadovy de Mitcheson, Y., Sumaila, U. R., Williams, M., Xue, G., Ye, Y., Zhang, W., Zhou, Y., Zhuang,  
525 P., and Naylor, R. L.: Opportunity for marine fisheries reform in China, *Proc Natl Acad Sci U S A*,  
526 114, 435-442, <https://doi.org/10.1073/pnas.1616583114>, 2017.
- 527 Carballeira Braña, C. B., Cerbule, K., Senff, P., and Stolz, I. K.: Towards environmental sustainability in  
528 marine Finfish aquaculture, *Frontiers in Marine Science*, 8,  
529 <https://doi.org/10.3389/fmars.2021.666662>, 2021.
- 530 Carboni, S., Clegg, S. H., and Hughes, A. D.: The use of biorefinery by-products and natural detritus as  
531 feed sources for oysters (*Crassostrea gigas*) juveniles, *Aquaculture*, 464, 392-398,  
532 <https://doi.org/10.1016/j.aquaculture.2016.07.021>, 2016.
- 533 Chen, C. L. and Qiu, G. H.: The long and bumpy journey: Taiwans aquaculture development and  
534 management, *Marine Policy*, 48, 152-161, <https://doi.org/10.1016/j.marpol.2014.03.026>, 2014.
- 535 Chen, Y. S., Beveridge, M., Telfer, T. C., and Roy, W. J.: Nutrient leaching and settling rate characteristics  
536 of the faeces of Atlantic salmon (*Salmo salar* L.) and the implications for modelling of solid waste  
537 dispersion, *Journal of Applied Ichthyology*, 19, 114-117, [https://doi.org/10.1046/j.1439-](https://doi.org/10.1046/j.1439-0426.2003.00449.x)  
538 [0426.2003.00449.x](https://doi.org/10.1046/j.1439-0426.2003.00449.x), 2003.



- 539 Chopin, T., Cooper, J. A., Reid, G., Cross, S., and Moore, C.: Open-water integrated multi-trophic  
540 aquaculture: environmental biomitigation and economic diversification of fed aquaculture by  
541 extractive aquaculture, *Reviews in Aquaculture*, 4, 209-220, [https://doi.org/10.1111/j.1753-](https://doi.org/10.1111/j.1753-5131.2012.01074.x)  
542 [5131.2012.01074.x](https://doi.org/10.1111/j.1753-5131.2012.01074.x), 2012.
- 543 Chopin, T., Buschmann, A. H., Halling, C., Troell, M., Kautsky, N., Neori, A., Kraemer, G. P., Zertuche-  
544 González, J., Yarish, C., and Neefus, C.: Integrating seaweeds into marine aquaculture systems: A key  
545 toward sustainability, *Journal of Phycology*, 37, 975-986, [https://doi.org/10.1046/j.1529-](https://doi.org/10.1046/j.1529-8817.2001.01137.x)  
546 [8817.2001.01137.x](https://doi.org/10.1046/j.1529-8817.2001.01137.x), 2001.
- 547 Corner, R. A., Brooker, A. J., Telfer, T. C., and Ross, L. G.: A fully integrated GIS-based model of  
548 particulate waste distribution from marine fish-cage sites, *Aquaculture*, 258, 299-311,  
549 <https://doi.org/10.1016/j.aquaculture.2006.03.036>, 2006.
- 550 Cromey, C. J., Nickell, T. D., and Black, K. D.: DEPOMOD—modelling the deposition and biological  
551 effects of waste solids from marine cage farms, *Aquaculture*, 214, 211-239,  
552 [https://doi.org/10.1016/S0044-8486\(02\)00368-X](https://doi.org/10.1016/S0044-8486(02)00368-X), 2002.
- 553 Dai, M., Zhao, Y., Chai, F., Chen, M., Chen, N., Chen, Y., Cheng, D., Gan, J., Guan, D., Hong, Y., Huang,  
554 J., Lee, Y., Leung, K. M. Y., Lim, P. E., Lin, S., Lin, X., Liu, X., Liu, Z., Luo, Y.-W., Meng, F.,  
555 Sangmanee, C., Shen, Y., Uthaiapan, K., Wan Talaat, W. I. A., Wan, X. S., Wang, C., Wang, D., Wang,  
556 G., Wang, S., Wang, Y., Wang, Y., Wang, Z., Wang, Z., Xu, Y., Yang, J.-Y. T., Yang, Y., Yasuhara, M.,  
557 Yu, D., Yu, J., Yu, L., Zhang, Z., and Zhang, Z.: Persistent eutrophication and hypoxia in the coastal  
558 ocean, *Cambridge Prisms: Coastal Futures*, 1-71, <https://doi.org/10.1017/cft.2023.7>, 2023.
- 559 Diana, J. S., Egna, H. S., Chopin, T., Peterson, M. S., Cao, L., Pomeroy, R., Verdegem, M., Slack, W. T.,  
560 Bondad-Reantaso, M. G., and Cabello, F.: Responsible aquaculture in 2050: Valuing local conditions  
561 and human innovations will be key to success, *BioScience*, 63, 255-262,  
562 <https://doi.org/10.1525/bio.2013.63.4.5>, 2013.
- 563 FAO: FAO Yearbook: fishery and aquaculture statistics 2019, Rome. 2022.12.18 download,  
564 <https://doi.org/10.4060/cb7874t>, 2021.
- 565 Froelich, P. N.: Kinetic control of dissolved phosphate in natural rivers and estuaries: A primer on the  
566 phosphate buffer mechanism, *Limnology & Oceanography*, 33, 649-668,  
567 [https://doi.org/10.4319/lo.1988.33.4\\_part\\_2.0649](https://doi.org/10.4319/lo.1988.33.4_part_2.0649), 1988.
- 568 Gao, G., Gao, L., Jiang, M., Jian, A., and He, L.: The potential of seaweed cultivation to achieve carbon  
569 neutrality and mitigate deoxygenation and eutrophication, *Environmental Research Letters*, 17,  
570 014018, <https://doi.org/10.1088/1748-9326/ac3fd9>, 2021.
- 571 Gordon, D. C., Boudreau, P., Mann, K., Ong, J., Silvert, W., Smith, S., Wattayakorn, G., Wulff, F., and  
572 Yanagi, T.: LOICZ biogeochemical modelling guidelines, LOICZ Core Project, Netherlands Institute  
573 for Sea Research Yerseke1996.





- 574 Granada, L., Sousa, N., Lopes, S., and Lemos, M. F. L.: Is integrated multitrophic aquaculture the  
575 solution to the sectors' major challenges? - a review, *Reviews in Aquaculture*, 8, 283-300,  
576 <https://doi.org/10.1111/raq.12093>, 2016.
- 577 Guo, X. and Wong, G. T. F.: Carbonate chemistry in the Northern South China Sea Shelf-sea in June  
578 2010, *Deep Sea Research Part II: Topical Studies in Oceanography*, 117, 119-130,  
579 <https://doi.org/10.1016/j.dsr2.2015.02.024>, 2015.
- 580 Hasan, B., Putra, I., Suharman, I., and Iriani, D.: Evaluation of salted trash fish as a protein source  
581 replacing fishmeal in the diet for river catfish (*Hemibagrus nemurus*), *Aquaculture, Aquarium,  
582 Conservation & Legislation-International Journal of the Bioflux Society*, 9, 647-656, 2016.
- 583 He, Y., Xuan, J., Ding, R., Shen, H., and Zhou, F.: Influence of suspended aquaculture on hydrodynamics  
584 and nutrient supply in the coastal Yellow Sea, *Journal of Geophysical Research: Biogeosciences*, 127,  
585 <https://doi.org/10.1029/2021jg006633>, 2022.
- 586 Huang, D. R. and Ding, G. M.: Distribution feature and correlation analysis of COD in Sansha Bay,  
587 *Journal of Fujian Fisheries*, 36, 453-458, <https://doi.org/10.14012/j.cnki.fjsc.2014.06.006>, 2014.
- 588 Huang, T. H., Chen, C. A., Lee, J., Wu, C. R., Wang, Y. L., Bai, Y., He, X., Wang, S. L., Kandasamy, S.,  
589 Lou, J. Y., Tsuang, B. J., Chen, H. W., Tseng, R. S., and Yang, Y. J.: East China Sea increasingly gains  
590 limiting nutrient P from South China Sea, *Scientific Reports*, 9, 5648, [https://doi.org/10.1038/s41598-  
591 019-42020-4](https://doi.org/10.1038/s41598-019-42020-4), 2019.
- 592 Jiang, Z. B., Chen, Q. Z., Zeng, J. N., Liao, Y. B., Shou, L., and Liu, J.: Phytoplankton community  
593 distribution in relation to environmental parameters in three aquaculture systems in a Chinese  
594 subtropical eutrophic bay, *Marine Ecology Progress Series*, 446, 73-89,  
595 <https://doi.org/10.3354/meps09499>, 2012.
- 596 Labasque, T., Chaumery, C., Aminot, A., and Kergoat, G.: Spectrophotometric Winkler determination of  
597 dissolved oxygen: re-examination of critical factors and reliability, *Marine Chemistry*, 88, 53-60,  
598 <https://doi.org/10.1016/j.marchem.2004.03.004>, 2004.
- 599 Li, Lei, Y., Xie, H., and Lu, J.: Water pollution analysis and protection measures of drinking water source  
600 of Jiaocheng Section of Huotong River, *Journal of Hengshui University*, 16, 92-96,  
601 <https://doi.org/10.3969/j.issn.1673-2065.2014.01.029>, 2014a.
- 602 Li, H., Tang, H., Shi, X., Zhang, C., and Wang, X.: Increased nutrient loads from the Changjiang (Yangtze)  
603 River have led to increased Harmful Algal Blooms, *Harmful Algae*, 39, 92-101,  
604 <https://doi.org/10.1016/j.hal.2014.07.002>, 2014b.
- 605 Li, P., Deng, Y., Shu, H., Lin, K., Chen, N., Jiang, Y., Chen, J., Yuan, D., and Ma, J.: High-frequency  
606 underway analysis of ammonium in coastal waters using an integrated syringe-pump-based  
607 environmental-water analyzer (iSEA), *Talanta*, 195, 638-646,  
608 <https://doi.org/10.1016/j.talanta.2018.11.108>, 2019.



- 609 Lin, H.: Tidal characteristics in the Sansha Bay of Fujian, *Journal of Fujian Fisheries*, 36, 306-314,  
610 <https://doi.org/10.14012/j.cnki.fjsc.2014.04.003>, 2014.
- 611 Lin, H., An, B., Chen, Z., Sun, Z., Chen, H., Zhu, J., and Huang, L.: Distribution of summertime and  
612 wintertime temperature and salinity in Sansha Bay, *Journal of Xiamen University*, 55, 349-356, 2016.
- 613 Lin, H., Chen, Z., Hu, J., Cucco, A., Sun, Z., Chen, X., and Huang, L.: Impact of cage aquaculture on  
614 water exchange in Sansha Bay, *Continental Shelf Research*, 188, 103963,  
615 <https://doi.org/10.1016/j.csr.2019.103963>, 2019.
- 616 Lin, H., Chen, Z., Hu, J., Cucco, A., Zhu, J., Sun, Z., and Huang, L.: Numerical simulation of the  
617 hydrodynamics and water exchange in Sansha Bay, *Ocean Engineering*, 139, 85-94,  
618 <https://doi.org/10.1016/j.oceaneng.2017.04.031>, 2017a.
- 619 Lin, H., Hu, J., Zhu, J., Cheng, P., Chen, Z., Sun, Z., and Chen, D.: Tide- and wind-driven variability of  
620 water level in Sansha Bay, Fujian, China, *Frontiers of Earth Science*, 11, 332-346,  
621 <https://doi.org/10.1007/s11707-016-0588-x>, 2017b.
- 622 Liu, W., Han, H., and Zhang, W.: Current situation analysis and further improvement strategy of Large  
623 Yellow Croaker industry in Ningde, *China Fisheries*, 555, 77-82, 2022.
- 624 Liu, Y.: Study on distributions and eutrophication of phosphorus in the Sansha Bay, *Environmental  
625 Protection Science*, 39, 43-47, <https://doi.org/10.16803/j.cnki.issn.1004-6216.2013.04.009>, 2013.
- 626 Marinho-Soriano, E., Panucci, R. A., Carneiro, M., and Pereira, D. C.: Evaluation of *Gracilaria caudata*  
627 *J. Agardh* for bioremediation of nutrients from shrimp farming wastewater, *Bioresource Technology*,  
628 100, 6192-6198, <https://doi.org/10.1016/j.biortech.2009.06.102>, 2009.
- 629 Martin-Jézéquel, V., Hildebrand, M., and Brzezinski, M. A.: Silicon metabolism in diatoms: Implications  
630 for growth, *Journal of Phycology*, 36, 821-840, <https://doi.org/10.1046/j.1529-8817.2000.00019.x>,  
631 2003.
- 632 Martínez-Porchas, M. and Martínez-Cordova, L. R.: World aquaculture: environmental impacts and  
633 troubleshooting alternatives, *Scientific World Journal*, 2012, 389623,  
634 <https://doi.org/10.1100/2012/389623>, 2012.
- 635 Nederlof, M. A. J., Verdegem, M. C. J., Smaal, A. C., and Jansen, H. M.: Nutrient retention efficiencies  
636 in integrated multi-trophic aquaculture, *Reviews in Aquaculture*, 14, 1194-1212,  
637 <https://doi.org/10.1111/raq.12645>, 2021.
- 638 Olsen, Y. and Olsen, L.: Environmental impact of aquaculture on coastal planktonic ecosystems,  
639 *Fisheries for global welfare and environment. Memorial book of the 5 th World Fisheries Congress*  
640 2008,
- 641 Qi, Z., Shi, R., Yu, Z., Han, T., Li, C., Xu, S., Xu, S., Liang, Q., Yu, W., Lin, H., and Huang, H.: Nutrient  
642 release from fish cage aquaculture and mitigation strategies in Daya Bay, southern China, *Marine  
643 Pollution Bulletin*, 146, 399-407, <https://doi.org/10.1016/j.marpolbul.2019.06.079>, 2019.



- 644 Redfield, A. C., Ketchum, B. H., and Richards, F. A.: The influence of organisms on the composition of  
645 sea-water, *The sea: ideas and observations on progress in the study of the seas*, Wiley Interscience:  
646 New York 1963.
- 647 Rios-Yunes, D., Tiano, J. C., van Rijswijk, P., De Borger, E., van Oevelen, D., and Soetaert, K.: Long-  
648 term changes in ecosystem functioning of a coastal bay expected from a shifting balance between  
649 intertidal and subtidal habitats, *Continental Shelf Research*, 254, 104904,  
650 <https://doi.org/10.1016/j.csr.2022.104904>, 2023.
- 651 Schneider, O., Sereti, V., Eding, E. H., and Verreth, J. A. J.: Analysis of nutrient flows in integrated  
652 intensive aquaculture systems, *Aquacultural Engineering*, 32, 379-401,  
653 <https://doi.org/10.1016/j.aquaeng.2004.09.001>, 2005.
- 654 Shan, L., Zhang, L., Fang, J., Shao, X., and Hu, Y.: Experiment and extension of main compound feed  
655 for fish culture in Southern Zhejiang seawater cages, *Fisheries Science & Technology Information*, 45,  
656 296-300, <https://doi.org/10.16446/j.cnki.1001-1994.2018.05.010>, 2018.
- 657 Skriptsova, A. V. and Miroshnikova, N. V.: Laboratory experiment to determine the potential of two  
658 macroalgae from the Russian Far-East as biofilters for integrated multi-trophic aquaculture (IMTA),  
659 *Bioresource Technology*, 102, 3149-3154, <https://doi.org/10.1016/j.biortech.2010.10.093>, 2011.
- 660 Song, Y., Li, M., Fang, Y., Liu, X., Yao, H., Fan, C., Tan, Z., Liu, Y., and Chen, J.: Effect of cage culture  
661 on sedimentary heavy metal and water nutrient pollution: Case study in Sansha Bay, China, *Science*  
662 *of Total Environment*, 899, 165635, <https://doi.org/10.1016/j.scitotenv.2023.165635>, 2023.
- 663 Subasinghe, R., Soto, D., and Jia, J.: Global aquaculture and its role in sustainable development, *Reviews*  
664 *in Aquaculture*, 1, 2-9, <https://doi.org/10.1111/j.1753-5131.2008.01002.x>, 2009.
- 665 Sugiura, S. H., Marchant, D. D., Kelsey, K., Wiggins, T., and Ferraris, R. P.: Effluent profile of  
666 commercially used low-phosphorus fish feeds, *Environmental Pollution*, 140, 95-101,  
667 <https://doi.org/10.1016/j.envpol.2005.06.020>, 2006.
- 668 Verdegem, Eding, Rooij, and Verreth: Comparison of effluents from pond and recirculating production  
669 systems receiving formulated diets, *World Aquaculture*, 30, 28-33, 1999.
- 670 Wang, C., Sun, Q., Jiang, S., and Wang, J.: Evaluation of pollution source of the bays in Fujian Province,  
671 *Procedia Environmental Sciences*, 10, 685-690, <https://doi.org/10.1016/j.proenv.2011.09.110>, 2011.
- 672 Wang, C. D. and Olsen, Y.: Quantifying regional feed utilization, production and nutrient waste emission  
673 of Norwegian salmon cage aquaculture, *Aquaculture Environment Interactions*, 15, 231-249,  
674 <https://doi.org/10.3354/aei00463>, 2023.
- 675 Wang, G., Han, A., Chen, L., Tan, E., and Lin, H.: Fluxes of dissolved organic carbon and nutrients via  
676 submarine groundwater discharge into subtropical Sansha Bay, China, *Estuarine, Coastal and Shelf*  
677 *Science*, 207, 269-282, <https://doi.org/10.1016/j.ecss.2018.04.018>, 2018.
- 678 Wang, X., Olsen, L. M., Reitan, K. I., and Olsen, Y.: Discharge of nutrient wastes from salmon farms:



679 environmental effects, and potential for integrated multi-trophic aquaculture, *Aquaculture*  
680 *Environment Interactions*, 2, 267-283, <https://doi.org/10.3354/aei00044>, 2012.

681 Wang, Y., Song, Z., Jiang, C., Kong, J., and Liu, Q.: Numerical simulation and environmental research  
682 of bay in Fujian Province: Sansha Bay, China Ocean Press, Beijing2009.

683 Wei, Z., You, J., Wu, H., Yang, F., Long, L., Liu, Q., Huo, Y., and He, P.: Bioremediation using *Gracilaria*  
684 *lemneciformis* to manage the nitrogen and phosphorous balance in an integrated multi-trophic  
685 aquaculture system in Yantian Bay, China, *Marine Pollution Bulletin*, 121, 313-319,  
686 <https://doi.org/10.1016/j.marpolbul.2017.04.034>, 2017.

687 Wu, H., Huo, Y., Hu, M., Wei, Z., and He, P.: Eutrophication assessment and bioremediation strategy  
688 using seaweeds co-cultured with aquatic animals in an enclosed bay in China, *Marine Pollution*  
689 *Bulletin*, 95, 342-349, <https://doi.org/10.1016/j.marpolbul.2015.03.016>, 2015.

690 Xie, B., Huang, J., Huang, C., Wang, Y., Shi, S., and Huang, L.: Stable isotopic signatures ( $\delta^{13}C$  and  
691  $\delta^{15}N$ ) of suspended particulate organic matter as indicators for fish cage culture pollution in Sansha  
692 Bay, China, *Aquaculture*, 522, 735081, <https://doi.org/10.1016/j.aquaculture.2020.735081>, 2020.

693 Xu, J. and Xu, Z.: Seasonal succession of zooplankton in Sansha Bay, Fujian, *Acta Ecologica Sinica*, 33,  
694 1413-1424, 2013.

695 Yan, S. and Cao, P.: Mineral characteristics of Sansha Bay and its sediment resources, *Journal of*  
696 *Oceanography in Taiwan Strait*, 16, 128-134, 1997.

697 Yang, J., Wu, D., and Lin, X.: On the dynamics of the South China Sea Warm Current, *Journal of*  
698 *Geophysical Research*, 113, <https://doi.org/10.1029/2007jc004427>, 2008.

699 Yang, Y. F., Fei, X. G., Song, J. M., Hu, H. Y., Wang, G. C., and Chung, I. K.: Growth of *Gracilaria*  
700 *lemneciformis* under different cultivation conditions and its effects on nutrient removal in Chinese  
701 coastal waters, *Aquaculture*, 254, 248-255, <https://doi.org/10.1016/j.aquaculture.2005.08.029>, 2006.

702 Zhai, W.-D., Chen, J.-F., Jin, H.-Y., Li, H.-L., Liu, J.-W., He, X.-Q., and Bai, Y.: Spring carbonate  
703 chemistry dynamics of surface waters in the northern East China Sea: Water mixing, biological uptake  
704 of  $CO_2$ , and chemical buffering capacity, *Journal of Geophysical Research: Oceans*, 119, 5638-5653,  
705 <https://doi.org/10.1002/2014jc009856>, 2014.

706 Zhao, Y., Liu, J., Uthaiapan, K., Song, X., Xu, Y., He, B., Liu, H., Gan, J., and Dai, M.: Dynamics of  
707 inorganic carbon and pH in a large subtropical continental shelf system: Interaction between  
708 eutrophication, hypoxia, and ocean acidification, *Limnology and Oceanography*,  
709 <https://doi.org/10.1002/lno.11393>, 2020.

710 Zheng, Q. H.: Physical and chemical variations and eutrophication status in important aquaculture waters  
711 of Sansha Bay, *Journal of Applied Oceanography*, 36, 24-30, 2017.

712

713